A&A 441, 615–629 (2005)
DOI: 10.1051/0004-6361:20052988

Astronomy & Astrophysics

Constraining fundamental stellar parameters using seismology

Application to α Centauri AB

A. Miglio and J. Montalbán

Institut d'Astrophysique et de Géophysique de l'Université de Liège, Allée du 6 Août 17, 4000 Liège, Belgium
e-mail: miglio@astro.ulg.ac.be

Received 4 March 2005 / Accepted 1 June 2005

Abstract. We apply the Levenberg-Marquardt minimization algorithm to seismic and classical observables of the αCen binary system in order to derive the fundamental parameters of αCenA+B, and to analyze the dependence of these parameters on the chosen observables, on their uncertainty, and on the physics used in stellar modelling. We show that while the fundamental stellar parameters do not depend on the treatment of convection adopted (Mixing Length Theory – MLT – or "Full Spectrum of Turbulence" – FST), the age of the system depends on the inclusion of gravitational settling, and is deeply biased by the small frequency separation of component B. We try to answer the question of the universality of the mixing length parameter, and we find a statistically reliable dependence of the α-parameter on the HR diagram location (with a trend similar to the predictions based on 2-D simulations). We propose the frequency separation ratios as better observables to determine the fundamental stellar parameters, and to use the large frequency separation and frequencies to extract information about the stellar structure. The effects of diffusion and equation of state on the oscillation frequencies are also studied, but present seismic data do not allow their determination.

Key words. stars: oscillations – stars: interiors – stars: fundamental parameters – stars: individual: α Cen

1. Introduction

α Cen AB is the binary system closest to the Earth (d = 1.34 pc). It shows an eccentric orbit (e = 0.519) with a period of almost 80 years (Pourbaix et al. 2002). αCen A is a G2V star and αCen B a K1V one, sligthly hotter and cooler respectively than the Sun. Thanks to the high apparent brightness (V_A = −0.01 and V_B = 1.33) and to the large parallax of the components, their stellar parameters are among the best known of any star except the Sun. The binarity, their well determined characteristics and the solar-like oscillations detected in both stars, provide a unique opportunity to test our knowledge on stellar evolution in conditions slightly different from the solar one.

As a consequence, a great number of theoretical studies dealing with αCen has been published since the one by Flannery & Ayres (1978) (see Eggenberger et al. 2004, for a comprehensive review). Before the definitive identification of p-mode frequencies in the αCen A power spectrum by Bouchy & Carrier (2002), the uncertainty in the parallax (and therefore in the masses) and in the chemical composition did not allow an unambiguous determination of stellar parameters. Some controversial results came up concerning, for instance, the universality or not of the mixing-length parameter (α) describing the stellar convection (Noels et al. 1991; Edmonds et al. 1992; Lydon et al. 1993; Neuforge 1993; Morel et al. 2000; Fernandes & Neuforge 1995; Guenther & Demarque 2000); the role of the chemical composition on discriminating between these two possibilities (Fernandes & Neuforge 1995), and on the presence or not of a convective core, and its effect on the age of the system (Guenther & Demarque 2000). Some efforts (Brown et al. 1994; Guenther & Demarque 2000; Morel et al. 2000) were also devoted to study the capability of solar-like oscillations expected in αCen (Kjeldsen & Bedding 1995) to constrain the fundamental stellar parameters and the physics included in stellar models.

In addition to the p-mode identification by Bouchy & Carrier (2002), Pourbaix et al. (2002) improved the precision of the orbital parameters and, adopting the parallax derived by Söderhjelm (1999), provided very precise masses for αCen A and B. These high quality data stimulated new calibrations of the system by Thévenin et al. (2002) and Thoul et al. (2003). The two teams reached different results. While Thévenin et al. (2002) could not fit the seismic data without changing the masses more than 4σ with respect to Pourbaix's data, the second group fitted the αCen A p-mode spectrum and the spectroscopic constraints using a single value of mixing length parameter, and with the new values for the masses.

Interferometric measurements with VINCI/VLTI by Kervella et al. (2003) have provided high precision values of

the angular diameter of αCen A and B, and new observations by Carrier & Bourban (2003) have allowed to identify p-mode frequencies also in the B component. These new constraints have been used by Eggenberger et al. (2004). Their calibration, based on a grid of models obtained by varying the mixing-length parameters, the chemical composition, and the age, leads to a stellar model in good agreement with the astrometric, photometric, spectroscopic and asteroseismic data, and they assert that *"the global parameters of the αCen system are now firmly constrained to an age of $t = 6.52 \pm 0.30$ Gyr, an initial helium mass fraction $Y_i = 0.275 \pm 0.010$ and an initial metallicity $(Z/X)_i = 0.0434 \pm 0.0020$"* and that *"the mixing length parameter α of the B component is larger than the one of the A component"*. These results are quantitatively consistent with those obtained by Thoul et al. (2003), nevertheless, both groups have performed the calibration assuming a given, but different, "physics".

The aim of this work is to study, following the theoretical analysis of the utility of seismology to constrain fundamental parameters made by Brown et al. (1994), the dependence of the set of parameters obtained by fitting the observables, on the details of the fitting procedure. That is: i) the kind of constraints included in the χ^2 functional that drives the fitting procedure, as well as other effects of their uncertainties, and ii) the physics included in the stellar evolution theory. Only in this way we will be able to provide an estimation of the uncertainty in the obtained set of stellar parameters, and to evaluate the degree at which the present data precision can constrain the physics in stellar evolution models.

To do that, and also with the prospect of dealing with a great quantity of seismic data from spatial missions such as MOST (Matthews 1998) and COROT (Baglin & The COROT Team 1998) and from new generation spectrograph such as HARPS (Bouchy 2002), we have implemented a non-linear fitting algorithm that performs a simultaneous least-square adjustment of all the observable characteristics, the classical and the seismic features.

The fitting method is described in Sect. 2. In Sect. 3 we discuss the different sets of classical and seismic observables that will be included in our χ^2 quality function. The physics included in the stellar evolutionary code is summarized in Sect. 4. The results of these different combinations of observables and of different physics are presented and discussed in Sect. 5. A special effort has been devoted to the problem of stellar convection (Sect. 5.2). We will try to answer to the question about the universality of the mixing-length parameter, and to study the effect of different convection treatments. With respect to the convection modelling, a controversial result was obtained by Morel et al. (2000); they reached different ages depending on whether they used the classical MLT theory (Böhm-Vitense 1958), or the FST theory by Canuto & Mazzitelli (1991, 1992, hereafter CM91, CM92). Hence, we performed different calibrations changing the convection treatment (FST or MLT), as well as different MLT calibrations either with a unique or different α values for each component. The effects of using different equation of state, including gravitational settling or not, and adopting a different solar mixture are discussed in Sect. 5.3. Finally, results and conclusions are summarized in Sect. 6.

2. Calibration method

Usually the approach to analyze stellar oscillation data is standard: i) several stellar models that bracket the known observational constraints (typically composition, mass, luminosity, and effective temperature) are computed; ii) p-mode oscillation frequencies are calculated for the models; and iii) the model oscillation spectra are compared with the observed one. We believe that a different approach is needed, so that asteroseismology is directly included in the calibration procedure and the results are not biased by a limited/subjective exploration of the parameter space or strongly depent on an initial guess of the model parameters.

The development and use of objective and efficient procedures to fit stellar models to observations has become of evident utility in particular since seismic constraints are included in the modelling (see e.g. Brown et al. 1994).

Guenther & Brown (2004) have proposed a method that quantifies at which degree the oscillation spectra as obtained from a grid of models parametrised in mass, age and composition reproduce the observations. Models providing a minimum in the χ^2, defined by the differences between the theoretical and observational frequencies, are selected for an additional inspection in a finer grid. As noted by Guenther & Brown (2004) the first problem in this kind of approach is its computational cost. Moreover the direct fit of the oscillation spectra implies a good knowledge of the surface layers of the star, as that strongly affects the exact frequency values. Guenther & Brown (2004) quantify the uncertainty in the theoretical frequencies due to our poor modelling of the external layers by using the discrepancies between observed and theoretical solar frequencies. But, how good is this estimation for stars with different superficial gravity, chemical composition and age? On the other hand, Eggenberger et al. (2004) use the aforementioned conventional approach, and only in a second and a third phase take into account the asteroseismic data, first the large and small frequency separations ($\Delta\nu$, $\delta\nu$), and then the frequencies.

Here we propose a calibration method that finds the parameters of the system by the minimization of a χ^2 functional including at the same time classical and asteroseismic observables. The parameters of the models are, as usual, the mass, initial chemical composition, age, parameter(s) of convection α. The observables could be chosen among the masses, $T_{\rm eff}$, L, R, [Fe/H], $\Delta\nu$, $\delta\nu$ (or combinations of these frequency differences). Of course, αCen being a binary system, the same initial chemical composition and age have to be assumed when calibrating components A and B.

We define a quality function measuring the distance between models and observations, that is, a goodness-of-fit measurement by:

$$\chi^2 = \sum_{i=1}^{N_{\rm o}} \frac{(O_i^{\rm obs} - O_i^{\rm theo})^2}{(\sigma_i^{\rm obs})^2} \qquad (1)$$

where $O_i^{\rm obs}$, $\sigma_i^{\rm obs}$ and $O_i^{\rm theo}$ are respectively the observed value, observational uncertainty and theoretical prediction of each of the $N_{\rm o}$ (A+B components) observables considered.

The choice of the observables included in the objective function is thoroughly described in Sect. 3.

In the general case of a binary system the model that generates the observables and their derivatives has seven free parameters (or six if $\alpha_A = \alpha_B$). The most substantial part of the model consists of a stellar evolution code (CLES, see Sect. 4) which takes as inputs the masses of each component (M_A, M_B), the initial chemical composition of the system (Y, Z), the age and the convection mixing-length parameters (α_A, α_B), that in general are assumed to be different for the two stars.

We compute oscillation frequencies for the models by solving the equations of adiabatic oscillations (OSC), and determine $\langle \Delta\nu \rangle$ and $\langle \delta\nu \rangle$ for the degrees $\ell = 0, 1, 2, 3$. This is not done by a least square fit to the computed frequencies, based on the asymptotic properties of low degree modes, but by making the average of the theoretical separations in the domain of observed radial order n ($n = 15-25$, for αCen A, and $n = 17-27$ for αCen B). The observed average separations have been determined from observed frequencies in the same way.

For each component the evolution code provides the stellar luminosity, the radius and the effective temperature, as well as the model quantities required in the subsequent calculations of the oscillation frequencies. In the calibration process, the derivatives of the observable quantities are obtained varying each of the parameters (M_A, M_B, Z, Y, α_A, α_B, and the age). We do not derive colors or visual magnitudes, and we do not include orbital elements such as apparent semi-major axis (a'), orbital period (P_{orb}) or parallax. We assume the parallax as determined by Söderhjelm (1999) and the values of observables based on it. The masses, however, are considered as parameters and also as observable quantities in our calibrations.

In the calibration of a binary system the large number of variables involved, both in terms of model parameters and observables, suggests the use of a least-squares based fitting procedure. This is particularly useful in this kind of calibration as we fit at the same time classical and seismological observables without first making a selection based on the HR location of the system.

As shown in Brown et al. (1994) the observable quantities depend on the parameters in a complex way: stellar evolution is not a linear problem. Most of the observables are influenced by several parameters, and hence the connection between observables and parameters that could conceptually seem to us the simplest one will not always provide the correct results.

2.1. Optimization algorithm

We use the gradient-expansion algorithm known as Levenberg-Marquardt method. This algorithm combines the advantages of an expansion method, i.e. rapid convergence close to the minima, with those of the gradient-search, that is, a rapid approach to a far away minimum. This method has as well the strong advantage of being reasonably insensitive to the starting values of the parameters.

At each step the fitting function is linearized calculating numerical derivatives (centered differences) of the observables with respect to each model parameter. The displacement in the parameter space, leading to a lower value of χ^2, is calculated following the prescription of Bevington & Robinson (2003), pp. 161−164 and the iterative procedure is ended when χ^2 no longer changes more than 2%. In calibrations with M_A, M_B, Z, Y, α_A, α_B, and the age as model parameters, convergence is typically achieved in 3−4 iterations and at each of them the computation of 16 evolutionary tracks is needed to evaluate centered derivatives. The result of such a local minimization could be sensitive to the initial guess of the parameters; therefore, in order to get a more reliable final solution we perform several runs starting from different points in the parameter space. The effect we find is limited to a variation of the number of iterations needed to reach the minimum χ^2, whereas the final parameters of the system differ much less than their uncertainty. On the other hand, building a 6-dimensional dense grid of models seems impractical considering the aim of evaluating the effects of using different physical prescriptions in our models (e.g. different equation of state, different metal mixture etc.).

It is sometimes nonetheless possible to make fairly direct connections between the observables and the parameters, particularly when one observable is much better determined than the rest. The solution is determined by the parameter that is known with very small uncertainty. The uncertainties in the parameters for these fits are calculated from the diagonal terms in the error matrix (inverse of curvature matrix in the parameter space) and are, in general considerably larger than the uncertainties obtained in the grid- and gradient-search methods. The latter are obtained by finding the change in each parameter to produce as change of χ^2 of 1 from the minimum values, without re-optimizing the fit, while there is a strong suggestion that correlations among the parameters play an important role in fitting (see e.g. Bevington & Robinson 2003).

3. The choice of the observational constraints

3.1. Non-asteroseismic constraints

Due to the proximity of the αCen binary system, the precision on the measurement of its trigonometric parallax is potentially very high. Unfortunately, some discrepancies have appeared among the most recent published values (see Table 10 in Kervella et al. 2003). Guenther & Demarque (2000) studied the uncertainty in the stellar parameters due to the different parallax values. This, indeed affects the determination of mass, luminosity and radius. Following Eggenberger et al. (2004) we adopt $\pi = 747.1 \pm 1.2$ mas (Söderhjelm 1999) and, therefore, the corresponding mass values determined by Pourbaix et al. (2002): ($M_A = 1.105 \pm 0.007\ M_\odot$, $M_B = 0.934 \pm 0.006\ M_\odot$) and the radii: ($R_A = 1.224 \pm 0.003\ R_\odot$; $R_B = 0.863 \pm 0.005\ R_\odot$) (Kervella et al. 2003).

As in the case of the parallax, there is a large scatter in the published values of other quantities, such as T_{eff}, luminosity, and metallicity. We decided to use the same values adopted by Eggenberger et al. (2004) in order to have a reference model. Eggenberger et al. (2004) took as T_{eff} for the component A a value to encompass those given by two spectroscopic determinations, the one from Neuforge-Verheecke & Magain (1997) ($T_{effA} = 5830 \pm 30$ K, $T_{effB} = 5255 \pm 50$ K),

Table 1. Non-asteroseismic constraints. References(1): Eggenberger et al. (2004); (2): Thoul et al. (2003).

	A	B	Ref.
$M/M_\odot$	1.105 ± 0.007	0.934 ± 0.006	(1)
$T_{\rm eff}$	5810 ± 50	5260 ± 50	(1)
$R/R_\odot$	1.224 ± 0.003	0.863 ± 0.005	(1)
$L/L_\odot$	1.522 ± 0.030	0.503 ± 0.020	(1)
Z/X	0.039 ± 0.006	0.039 ± 0.006	(2)

and the one by Morel et al. (2000) based on a re-analysis of Chmielewski et al. (1992) spectra ($T_{\rm eff\,A}$ = 5790 ± 30 K, $T_{\rm eff\,B}$ = 5260 ± 50 K), used respectively in the αCen calibrations by Thoul et al. (2003) and Thévenin et al. (2002). We will use the effective temperature as constraint in our minimization method only in one of the calibrations (A1t, B1t, in Table 2), since the precise determination of the radius provides a narrower domain in the space of observable quantities. The luminosity values adopted by Eggenberger et al. (2004) come from a new and weighted calibration of previous Geneva photometric data, where they have also coherently taken into account the effective temperatures and the parallax. These values cover the domain considered by Thévenin et al. (2002) that considered an error bar twice smaller, and a lower luminosity for the component B. The luminosity values, directly determined from the adopted radius and effective temperature, are in very good agreement with the those determined by Eggenberger et al. (2004): $L_{\rm A}/L_\odot$ = 1.518 ± 0.06, $L_{\rm B}/L_\odot$ = 0.507 ± 0.025. On the other hand, the values determined by Pijpers (2003) for $L_{\rm A}$ are much larger and only marginally overlap the values considered here.

The precise values of masses and radius provide also precise values of the surface gravity for both stars: $\log g_{\rm A}$ = 4.305 ± 0.005 and $\log g_{\rm B}$ = 4.536 ± 0.008, while the spectroscopic values determined by Neuforge-Verheecke & Magain (1997) are $\log g_{\rm A} = 4.34 \pm 0.05$ and $\log g_{\rm B} = 4.51 \pm 0.08$. These values were used by Thoul et al. (2003) to fix the luminosity domain, leading to higher central values and to larger error bars with respect to those determined by Eggenberger et al. (2004) and Thévenin et al. (2002).

For the metallicity of both components there is also no complete agreement in the literature: $[{\rm Fe/H}]_{\rm A}$ = 0.20 ± 0.02, and $[{\rm Fe/H}]_{\rm B}$ = 0.23 ± 0.03 from Morel et al. (2000), and $[{\rm Fe/H}]_{\rm A}$ = 0.25 ± 0.02, and $[{\rm Fe/H}]_{\rm B}$ = 0.24 ± 0.03 from Neuforge-Verheecke & Magain (1997). The uncertainty in the observable Z/X is quite large, if we take into account also the 10% in the $(Z/X)_\odot$. We have taken the value adopted by Thoul et al. (2003), that is Z/X = 0.039 ± 0.006, the same for both stars. The detailed abundance analysis of α Cen A and B carried out in Neuforge-Verheecke & Magain (1997) suggested no evidence for a different metal mixture relative to the sun, therefore all our models were computed assuming the solar mixture by Grevesse & Noels (1993), except for the calibration (A5, B5) in which we have considered the recently determined solar metal abundances (Asplund et al. 2004, 2005) that implies $(Z/X)_\odot$ = 0.0177.

The non-asteroseismic constraints used in this work are summarized in Table 1.

3.2. Seismic constraints

Solar-like oscillations generate periodic motions of the stellar surface with periods in the range of 3−30 min and with extremely small amplitudes. The frequency and amplitude of each oscillation mode depend on the physical condition prevailing in the layers crossed by the waves and provide a powerful seismological tool. Helioseismology led to major improvements in the knowledge of solar structure and to revision of the "standard solar model". The potential utility of seismology applied to other stars, in particular αCen, to constrain the stellar parameters was extensively studied in Brown et al. (1994), and also by Guenther & Demarque (2000).

Several groups have made thorough attempts to detect the signature of p-mode oscillations in αCen A, but their results were not confirmed. Only recently Bouchy & Carrier (2002), from high precision radial velocity measurements with the CORALIE echelle spectrograph have reported a clear detection of p-mode oscillation, and identified several modes between 1800 and 2900 μHz, and with an envelope amplitude of about 31 cm s^{-1}. Assuming that frequency modes $\nu_{n\ell}$ satisfy the simplified asymptotic relation (Tassoul 1980):

$$\nu_{\ell n} \approx \Delta\nu_0 \left(n + \frac{\ell}{2} + \epsilon \right) - \ell(\ell+1)\frac{\delta\nu_{02}}{6} \qquad (2)$$

and assuming the parameter ϵ near the solar one (1.5) they estimated: $\Delta\nu_0$ = 105.5 ± 0.1 μHz, $\delta\nu_{02}$ = 5.6 ± 0.7 μHz, ϵ = 1.40 ± 0.02 and identified 28 p-modes with degree $\ell = 0, 1, 2$ and order between n = 15 and n = 25.

Notice that the given errors come from the autocorrelation algorithm, but we must keep in mind that their frequency resolution is only 0.93 μHz, and that they derive an uncertainty in the frequency determination equal to 0.46 μHz. They also point out that an error of ±1.3 μHz could have been introduced at some identified mode frequency, that could explain the dispersion of mode frequency around the asymptotic relation. In particular, higher observational uncertainty could affect mainly the $\ell = 2$ modes that determine the value of $\delta\nu_{02}$ for the lower and higher frequency $\delta\nu_{02}(n = 16$ and 25).

Carrier & Bourban (2003) have also detected solar-like oscillations in the fainter component, αCen B. Only twelve frequencies, between 3000 and 4600 μHz, have been kept in the final list of identified p-modes, four of them with a detection level lower than 3σ, and it is recommended to take them with caution. As for component A the frequency resolution is 0.93 μHz. The large and small separations, determined by autocorrelation of the asymptotic relation, are respectively $\Delta\nu_0$ = 161.1 ± 0.1 μHz and $\delta\nu_{02}$ = 8.7 ± 0.8 μHz. The value derived for $\delta\nu_{02}$ comes from only few p-modes. In fact, from their frequency table is only possible to obtain two values: $\delta\nu_{02}(n = 21) = 10.0$ μHz and $\delta\nu_{02}(n = 23) = 7.0$ μHz. Carrier & Bourban (2003) expect a rotational splitting ∼0.3 μHz that, given the frequency resolution, could imply an increase of the uncertainty of frequencies for modes of degree $\ell = 1$ and $\ell = 2$.

New observations of this system by Kjeldsen & Bedding (2004) have confirmed the values determined by Bouchy & Carrier (2002) concerning the frequency separations of component A. However, component B with this new more precise data shows $\Delta\nu_0 = 161.4$ μHz and $\delta\nu_{02} = 10.1$ μHz. Our computations were done before these values were available, therefore, we will not take them into account in our calibration. Nevertheless, those values are reached and imposed by the other observables used in some of our calibrations (A3, B3), see Sect. 5.

How should these seismological observations be used to constrain our stellar models? The classical way is to use the large and small separations to characterize the power spectrum of solar-like oscillations. The standard asymptotic theory of stellar oscillations (Tassoul 1980) relates the averages values of high-radial order/low-degree small and large separations to conditions in the stellar core ($\delta\nu$) and to the mean density of the star ($\Delta\nu$). Recently Guenther & Brown (2004) and Metcalfe (2005) have proposed to use directly the p-mode frequencies as observables to constrain the stellar models.

Brown et al. (1994) theoretically analyzed the case in which the individual frequencies are included as observables. Their purpose was to illustrate the potential loss of information resulting from representing the spectra in terms of the large and small separations derived from the expected asymptotic behavior. The dominant source of frequency changes is very close to the stellar surface. It could be difficult to disentangle these effects from the uncertainties in the treatment of the physics of the outer layers, where non-adiabaticity and dynamics effects of convection have to be taken into account.

The oscillation frequencies, the large and small separations depend on the structure of both the inner and the outer layers of a star, so model fitting and testing techniques to probe the interior structure of the stars are dependent on our having a good understanding of the structure of the outer layers. But these are just the layers where our ignorance is greatest; non-adiabatic convection is important but not understood, the oscillations are non-adiabatic in the surface layers and the structure of real stellar atmosphere is poorly understood. For example the oscillation frequencies predicted by the reference solar models (S96) (Christensen-Dalsgaard et al. 1996) differ from the observed values up to 10 μHz at the higher end of the observed frequency range.

In a first step, we will include as seismic constraints in our fitting algorithm the combinations of frequencies: the large

$$\Delta\nu_{n,\ell} = \nu_{n,\ell} - \nu_{n-1,\ell}$$

and small

$$\delta\nu_{n,\ell} = \nu_{n,\ell} - \nu_{n-1,\ell+2}$$

frequency separations defined from the identified p-mode frequencies for both components.

As discussed in Christensen-Dalsgaard et al. (1995) and Di Mauro et al. (2003), care has to be taken when considering as a constraint in the modelling the large separation, as its averaged value at high frequencies could be influenced by near-surface effects as well. This is in fact the case when comparing

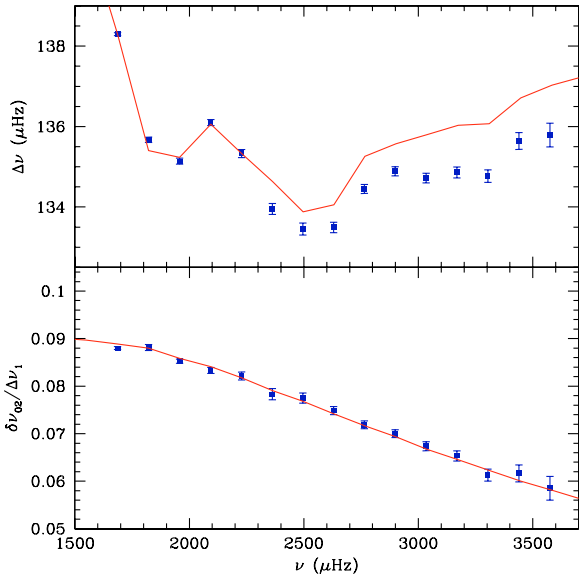

Fig. 1. Solar large frequency difference $\Delta\nu_{n,1}$ (*upper panel*) from standard seismic solar model S96 (Christensen-Dalsgaard et al. 1996) (solid line), compared to the observational solar large separation (dots) (Basu et al. 1997). *Lower panel*: as upper panel but for the ratio r_{02}.

the observed and the predicted low-degree large separations of the Sun (see Fig. 1), where the disagreement of the order of a μHz is related to a simplified treatment of the model outer layers.

With the aim of checking whether the calibration we perform considering $\langle\Delta\nu\rangle$ and $\langle\delta\nu\rangle$ is not biased by a simplified treatment of the outer structure in our models, we considered the effect on the calibration of choosing as seismic constraint r_{02}, the ratio between the small and large frequency separations defined by:

$$r_{02}(n) = \frac{\delta\nu_{n,0}}{\Delta\nu_{n,1}} = \frac{\nu_{n,0} - \nu_{n-1,2}}{\nu_{n,1} - \nu_{n-1,1}} \quad (3)$$

for 6 different orders n of the component A. This combination of frequencies, as presented in Roxburgh & Vorontsov (2003), is to a great accuracy independent of the outer layers of the star, and therefore represents a reliable indicator of the conditions in the deep stellar interior.

4. Stellar models

All stellar model sequences are calculated using the CLES code (Code Liégeois d'Evolution Stellaire). The opacity tables are those of OPAL96 (Iglesias & Rogers 1996) complemented at $T < 6000$ K with Alexander & Ferguson (1994) opacities. The relative mixture of heavier than helium elements, used in the opacity and equation of state tables, is the solar one according to Grevesse & Noels (1993). The nuclear energy generation routines are based on the cross sections by Caughlan & Fowler (1988) and screening factors from Salpeter (1954). CLES allows the choice between two equations of state: CEFF (Christensen-Dalsgaard & Däppen 1992) and OPAL01 (Rogers & Nayfonov 2002). Most of the models have been computed using OPAL01, but we have also made a

Table 2. Sets of parameters of fitted models. Meaning of numeric labels: 1 (fixed masses and $\Delta\nu$, $\delta\nu$ as seismic constraints); 2 (as 1 but with variable masses); 3 (as 2 but using $r_{02}(n)$ as seismic constraint); 4 (as 3 but including convective overshooting) and 5 (as 3 but using Asplund et al. 2005 instead of Grevese & Noels 1993). Meaning of alphabetic labels: nd (non diffusion models); f (FST convection treatment); e (CEFF EoS instead of OPAL01 one); c (a unique mixing-length parameter); ns (fit without seismic constraints); only for the case 1, t refers to effective temperature as constraint, and r to radius as constraint.

Model	Conv	Diff	EoS	fitting	$M/M_\odot$	ϵ	α	ϵ	Age	ϵ	Y_0	ϵ	Z_0	ϵ
A1t	MLT	Y	OPAL	$T_{\rm eff}$, $M_{\rm fix}$	1.105		1.99	0.11	7.0	0.5	0.273	0.016	0.0316	0.003
B1t	MLT	Y	OPAL	$\langle\Delta\nu\rangle$, $\langle\delta\nu\rangle$	0.934		2.22	0.07	7.0	0.5	0.273	0.016	0.0316	0.003
A1r	MLT	Y	OPAL	$M_{\rm fix}$	1.105		2.00	0.11	6.8	0.5	0.276	0.015	0.0325	0.003
B1r	MLT	Y	OPAL	$\langle\Delta\nu\rangle$, $\langle\delta\nu\rangle$	0.934		2.24	0.07	6.8	0.5	0.276	0.015	0.0325	0.003
A1nd	MLT	N	OPAL	$M_{\rm fix}$	1.105		1.84	0.10	7.1	0.6	0.265	0.015	0.0284	0.003
B1nd	MLT	N	OPAL	$\langle\Delta\nu\rangle$, $\langle\delta\nu\rangle$	0.934		1.99	0.05	7.1	0.6	0.265	0.015	0.0284	0.003
A1e	MLT	Y	CEFF	$M_{\rm fix}$	1.105		1.93	0.10	6.7	0.6	0.281	0.015	0.0324	0.003
B1e	MLT	Y	CEFF	$\langle\Delta\nu\rangle$, $\langle\delta\nu\rangle$	0.934		2.08	0.06	6.7	0.6	0.281	0.015	0.0324	0.003
A1-3	MLT	Y	OPAL	$M_{\rm fix}$,	1.105		1.86	0.06	6.0	0.4	0.277	0.017	0.0302	0.003
B1-3	MLT	Y	OPAL	$r_{02}(n)$	0.934		2.18	0.05	6.0	0.4	0.277	0.017	0.0302	0.003
A2	MLT	Y	OPAL	$M_{\rm var}$	1.104	0.006	1.96	0.11	6.4	0.6	0.282	0.016	0.0326	0.003
B2	MLT	Y	OPAL	$\langle\Delta\nu\rangle$, $\langle\delta\nu\rangle$	0.926	0.005	2.11	0.10	6.4	0.6	0.282	0.016	0.0326	0.003
A2c	MLT	Y	OPAL	$M_{\rm var}$ $\alpha_{\rm A}=\alpha_{\rm B}$	1.107	0.005	1.78	0.08	5.4	0.5	0.284	0.016	0.0305	0.003
B2c	MLT	Y	OPAL	$\langle\Delta\nu\rangle$, $\langle\delta\nu\rangle$	0.919	0.004	"	"	5.4	0.5	0.284	0.016	0.0305	0.003
A2f	FST	Y	OPAL	$M_{\rm var}$	1.105	0.006	0.77	0.05	6.4	0.6	0.282	0.016	0.0325	0.003
B2f	FST	Y	OPAL	$\langle\Delta\nu\rangle$, $\langle\delta\nu\rangle$	0.927	0.005	0.89	0.05	6.4	0.6	0.282	0.016	0.0325	0.003
A3	MLT	Y	OPAL	$M_{\rm var}$	1.110	0.006	1.90	0.07	5.8	0.2	0.284	0.014	0.0322	0.003
B3	MLT	Y	OPAL	$r_{02}(n)$	0.927	0.005	2.05	0.08	5.8	0.2	0.284	0.014	0.0322	0.003
A3c	MLT	Y	OPAL	$M_{\rm var}$, $\alpha_{\rm A}=\alpha_{\rm B}$	1.113	0.006	1.95	0.05	5.8	0.5	0.276	0.017	0.0317	0.003
B3c	MLT	Y	OPAL	$r_{02}(n)$	0.922	0.004	"	"	5.8	0.5	0.276	0.017	0.0317	0.003
A3$\alpha_\odot$	MLT	Y	OPAL	$M_{\rm var}$, $\alpha=\alpha_\odot$	1.114	0.006	1.91		5.7	0.2	0.283	0.010	0.0314	0.002
B3$\alpha_\odot$	MLT	Y	OPAL	$r_{02}(n)$	0.921	0.004	"		5.7	0.2	0.283	0.010	0.0314	0.002
A3f	FST	Y	OPAL	$M_{\rm var}$	1.110	0.006	0.74	0.03	5.8	0.2	0.285	0.015	0.0323	0.003
B3f	FST	Y	OPAL	$r_{02}(n)$	0.927	0.005	0.86	0.03	5.8	0.2	0.285	0.015	0.0323	0.003
A3nd	MLT	N	OPAL	$M_{\rm var}$	1.108	0.006	1.84	0.07	6.3	0.4	0.270	0.015	0.0281	0.003
B3nd	MLT	N	OPAL	$r_{02}(n)$	0.929	0.005	1.99	0.07	6.3	0.4	0.270	0.015	0.0281	0.003
A3e	MLT	Y	CEFF	$M_{\rm var}$	1.109	0.006	1.85	0.07	5.7	0.3	0.288	0.015	0.0322	0.003
B3e	MLT	Y	CEFF	$r_{02}(n)$	0.927	0.005	1.93	0.07	5.7	0.3	0.288	0.015	0.0322	0.003
A4	OV	Y	OPAL	$M_{\rm var}$	1.112	0.006	1.77	0.05	5.2	0.2	0.285	0.015	0.0299	0.003
B4	OV	Y	OPAL	$r_{02}(n)$	0.925	0.005	1.98	0.07	5.2	0.2	0.285	0.015	0.0299	0.003
A5	MLT	Y	OPAL	$M_{\rm var}$, A04 mix	1.109	0.006	1.74	0.06	5.9	0.3	0.280	0.013	0.0239	0.002
B5	MLT	Y	OPAL	$r_{02}(n)$	0.927	0.005	1.84	0.07	5.9	0.3	0.280	0.013	0.0239	0.002
Ans	MLT	Y	OPAL	$M_{\rm var}$,	1.105	0.007	2.40	0.33	8.9	1.8	0.259	0.021	0.0340	0.003
Bns	MLT	Y	OPAL	No Seismo	0.934	0.006	2.61	0.31	8.9	1.8	0.259	0.021	0.0340	0.003

calibration using CEFF to study the capability of seismology to constrain the EoS.

All our stellar models were obtained from evolutionary tracks including the pre-main sequence phase, and ending at ~9 Gyr. The stellar models have approximately 1200 shells, the last one corresponding to $T = T_{\rm eff}$ as determined using as boundary conditions those given by the Kurucz (1998) atmosphere models. Furthermore, for the computation of oscillations we have added atmospheric layers from $T = T_{\rm eff}$ up to $\tau = 10^{-4}$.

We have computed models where the convection is treated both using the Mixing Length Theory (MLT Böhm-Vitense 1958) with the formalism described in Cox & Giuli (1968), and the Full Spectrum of Turbulence (FST Canuto et al. 1996) with a formalism similar to the one used by Morel et al. (2000) or Bernkopf (1998). That means convective fluxes as given by Canuto et al. (1996), but another prescription of the scale length. The parameter α of the MLT and the corresponding in the FST are considered as free parameters of the model calibration, and the values obtained are compared with the values required in the solar calibration for the same physics.

Finally we have computed stellar models with and without gravitational settling of helium and metals. The microscopic diffusion formulation is that given by Thoul et al. (1994), solving the Burgers (1969) equations for H, He and Z and thus considering diffusion due both to thermal and concentration gradients. We also assume complete ionization and the effect of radiative acceleration is ignored. This assumption is completely justified for the precision of the models and for the masses considered (Turcotte et al. 1998).

5. Results

In Table 2 we list all the fits of the binary system αCen. The calibrations differ in the choice of the observables included in the objective function (χ^2) and in the used physics. The first

Table 3. Observable quantities predicted from the sets of parameters in Table 2.

Model	$M/M_\odot$	χ^2_{Ri}	$(Z/X)_s$	χ^2_{Ri}	$R/R_\odot$	χ^2_{Ri}	$T_{\rm eff}$	χ^2_{Ri}	$L/L_\odot$	χ^2_{Ri}	$\Delta\nu$	χ^2_{Ri}	$\delta\nu$	χ^2_{Ri}	χ^2_R
A1t	1.105		0.037	0.06	1.234		5764	0.17	1.508	0.04	105.7	0.01	4.95	0.66	1.52
B1t	0.934		0.039	0.00	0.874		5280	0.03	0.534	0.44	161.1	0.	9.22	0.1	
A1r	1.105		0.038	0.02	1.227	0.20	5770		1.498	0.13	106.5	0.52	5.07	0.53	2.80
B1r	0.934		0.041	0.00	0.872	0.67	5289		0.533	0.48	161.6	0.11	9.33	0.14	
A1nd	1.105		0.040	0.00	1.227	0.17	5780		1.508	0.05	106.6	0.56	5.34	0.27	2.27
B1nd	0.934		0.040	0.00	0.872	0.66	5258		0.521	0.17	161.7	0.13	9.60	0.24	
A1e	1.105		0.038	0.02	1.228	0.24	5772		1.500	0.10	106.5	0.46	5.16	0.43	2.64
B1e	0.934		0.041	0.01	0.872	0.66	5286		0.533	0.44	161.6	0.44	9.42	0.17	
A1-3	1.105		0.035	0.07	1.224	0.00	5767		1.488	0.16	106.5		5.77	0.99	2.08
B1-3	0.934		0.038	0.01	0.871	0.29	5315		0.543	0.51	161.6	0.04	9.85		
A2	1.104	0.00	0.039	0.01	1.226	0.13	5782		1.509	0.04	106.6	0.55	5.35	0.26	2.20
B2	0.926	0.32	0.042	0.01	0.870	0.38	5259		0.520	0.12	161.6	0.09	9.72	0.30	
A2c	1.107	0.01	0.036	0.07	1.227	0.22	5778		1.508	0.04	106.6	0.45	6.28	0.03	2.89
B2c	0.919	0.99	0.040	0.00	0.870	0.37	5210		0.501	0.00	161.0	0.00	10.54	0.69	
A2f	1.105	0.00	0.039	0.01	1.226	0.12	5784		1.510	0.03	106.4	0.32	5.35	0.27	1.80
B2f	0.927	0.28	0.041	0.01	0.869	0.28	5261		0.519	0.13	161.6	0.07	9.72	0.29	
A3	1.110	0.06	0.038	0.01	1.224	0.00	5791		1.512	0.01	106.6		5.87	0.94	1.46
B3	0.927	0.18	0.042	0.02	0.869	0.16	5259		0.518	0.07	161.4	0.03	10.16		
A3c	1.113	0.17	0.038	0.02	1.223	0.01	5819		1.540	0.04	106.8		5.77	0.87	1.67
B3c	0.922	0.40	0.041	0.00	0.870	0.16	5206		0.497	0.01	161.1	0.00	10.22		
A3$\alpha_\odot$	1.114	0.15	0.038	0.02	1.224	0.00	5807		1.529	0.00	106.8		5.94	0.75	1.60
B3$\alpha_\odot$	0.921	0.47	0.041	0.01	0.869	0.15	5190		0.491	0.04	160.7	0.02	10.35		
A3f	1.110	0.06	0.038	0.01	1.224	0.00	5790		1.511	0.02	106.5		5.85	0.92	1.40
B3f	0.927	0.16	0.042	0.01	0.868	0.12	5260		0.518	0.07	161.4	0.02	10.14		
A3nd	1.108	0.02	0.040	0.00	1.224	0.00	5795		1.516	0.01	106.5		5.90	0.95	1.31
B3nd	0.929	0.10	0.040	0.00	0.869	0.19	5240		0.511	0.02	161.6	0.04	10.16		
A3e	1.109	0.05	0.038	0.01	1.224	0.00	5792		1.514	0.01	106.6		5.89	0.95	1.45
B3e	0.927	0.16	0.042	0.01	0.869	0.17	5256		0.517	0.06	161.5	0.03	10.17		
A4	1.112	0.13	0.036	0.05	1.224	0.00	5782		1.503	0.05	106.7		5.99	1.16	1.96
B4	0.925	0.27	0.039	0.0	0.869	0.15	5275		0.524	0.13	161.5	0.02	10.56		
A5	1.109	0.04	0.028	0.02	1.224	0.00	5791		1.513	0.01	106.7		5.86	0.95	1.51
B5	0.927	0.17	0.030	0.01	0.869	0.20	5251		0.516	0.05	161.6	0.05	10.12		
Ans	1.105		0.039		1.224		5800		1.521		107.0		3.57		0.06
Bns	0.934		0.041		0.863		5238		0.502		164.3		8.27		

column in Table 2 identifies the models, the second, third and fourth columns describe the physics; the fifth one resumes the characteristic of the seismic and non-seismic constraints used in the calibration process, while all the following columns give the values of the parameters (and the uncertainty in each of them) providing in each case the minimum χ^2. The values of the observable quantities derived for each set of parameters is listed in Table 3. There, the last column χ^2_R is the the value of the "reduced" χ^2, defined as:

$$\chi^2_R = \frac{\chi^2}{N_o - N_p} \quad (4)$$

were N_o is the number of observables and N_p the number of model parameters.

In the three following subsections we shall analyze the effect of changing the non-seismic constraints, the seismic constraints and finally the physics used in the models, that is, a different treatment of convection, different equation of state, different solar mixture, models including or not gravitational settling, and the effect of considering overshooting in our models.

Figure 2 shows the HR location of each of these fitted models. We have indicated the error boxes in $T_{\rm eff}$ $\log L/L_\odot$, and radius, corresponding to 1σ (solid line), and 2σ (dashed-line).

5.1. Effect of classic and seismic observable quantities

A first calibration (A1r, B1r) was performed including in the χ^2 function the luminosity, the radii and the actual $(Z/X)_s$, as well as the average large and small frequency separations (computed as described in Sect. 2) for each component. The model parameters are the initial chemical composition (Y_0, Z_0), the mixing length parameters (α_A, α_B) and the age (τ). In this calibration we consider, following Eggenberger et al. (2004), that the masses are perfectly determined, and we assume the mass of each component to be fixed to its observational central value, as given Pourbaix et al. (2002). The parameters providing the minimum χ^2 are: $\tau = 6.8 \pm 0.5$ Gyr, $\alpha_A = 2.00$, $\alpha_B = 2.24$, $Y_0 = 0.276$ and $Z_0 = 0.0325$. We note that these results are in complete agreement with those obtained by Eggenberger et al. (2004): $\tau = 6.5 \pm 0.2$ Gyr, $Z_0 = 0.0302$, $Y_0 = 0.275$, and also

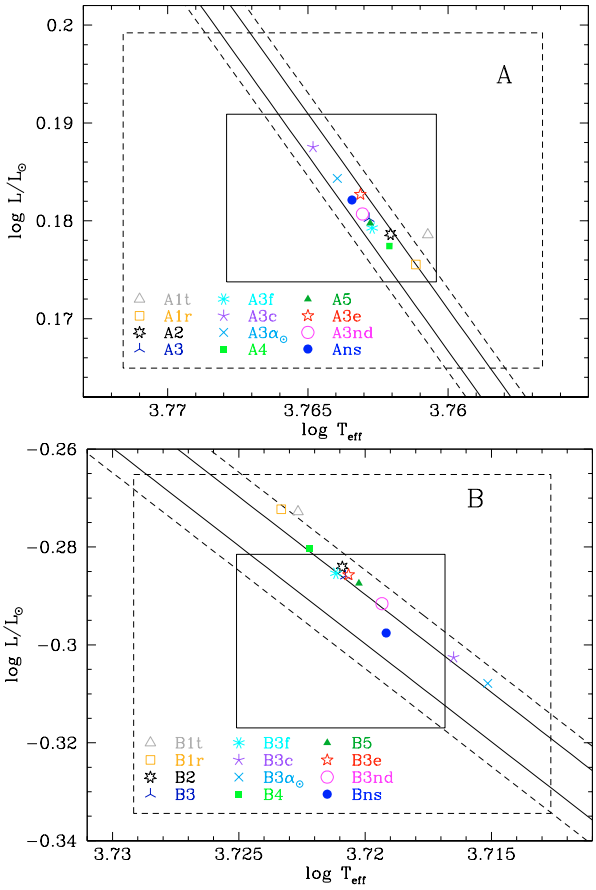

Fig. 2. HR diagram location of models with stellar parameters from differing fits. Labels corresponds to those in Tables 2, and 3. Upper and lower panel correspond respectively to components A and B. The error boxes for $T_{\rm eff}$, $\log L/L_\odot$, and radii correspond to 1σ (solid line) and 2σ (dashed-line)

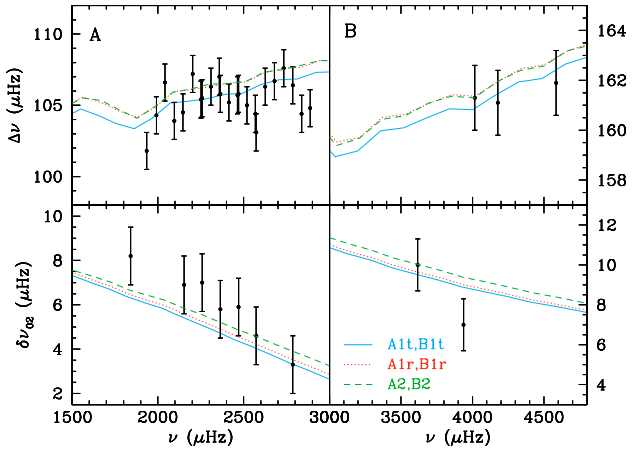

Fig. 3. Large (*upper panels*) and small (*lower panels*) separations for the A (*left*) and B (*right*) components of αCen system. Points represent the observational values with their error bars assuming an error in frequencies equal to 2σ. All these curves correspond to calibrations performed including in the χ^2 functional the average of the observational large and small separations, but different classical observational constraints: masses fixed to the value given by Pourbaix et al. (2002) and $T_{\rm eff}$ (solid lines); radii (dotted-lines); and masses variable as parameter and radii (dashed-lines). All the curves were computed from stellar models including gravitational settling, and MLT treatment of convection with two mixing length adjustable parameters. For clarity only $\ell = 1$ theoretical large separations are shown in the upper panels.

their value for the mixing-length parameter of αCen B is ~10% larger than $\alpha_{\rm A}$.

This agreement is not surprising, as similar observational constraints were considered. It strengthens the results obtained, since a different calibration procedure and different stellar evolution codes (with different equation of state, treatment of diffusion and treatment of sub-photospheric boundary conditions) were used, and it provides us with a good reference model to study the dependence of the calibrated stellar parameters on the choice of observable quantities and of the physics.

The observational values of the masses given by Pourbaix et al. (2002), though precisely determined, should be treated as observables and therefore introduced, with their error bars, in the definition of the χ^2 and allowed to be changed during the calibration. $M_{\rm A}$ and $M_{\rm B}$ are considered both as parameters and observables in a second set of fittings (A2, B2; A2f, B2f). The readjustment of parameters leads to a decrease of $M_{\rm B}$ which is 1.5σ smaller than the value determined by Pourbaix et al. (2002), and to a decrease of age ($\tau = 6.4 \pm 0.6$ Gyr instead of 6.8 ± 0.5 Gyr). The location of αCen B in the HR diagram has significantly improved compared with (A1r, B1r) (Fig. 2) and $\langle \Delta\nu_{\rm A} \rangle$ is also better reproduced (Fig. 3), leading to an overall lower $\chi^2_{\rm R}$ compared with the equivalent fitting with fixed masses.

Even including the stellar masses among the parameters, we are not able to improve significantly the fit of radii and large separations. Actually the large separation is strongly dependent on radius ($\Delta\nu \propto (M/R^3)^{1/2}$), and, given the high precision of radius data, the procedure privileges sets of parameters providing the radii within 1σ (for A), and 1.5σ (for B) to detriment of a too high large separation: $\Delta\nu_{\rm A}$ is always around 106.6 μHz instead of 105.5 μHz. In order to relax the constraints, we have performed a fitting including $T_{\rm eff}$ among the observables instead of the radii (A1t, B1t). This fitting provided a small $\chi^2_{\rm R}$ thanks to the good match of large separation values. However, the radii (not included in the χ^2 function) are systematically larger (by more than 2σ) than Kervella et al. (2003) ones. The large separation is very much affected by the external layers properties, such as either the description of the super-adiabatic region in the upper boundary of the convective zone, or the non-adiabatic processes (not taken into account either in the stellar models or in the oscillation code). An inspection of frequencies predicted for these models (Fig. 6) shows that even if the fit of $\Delta\nu_{\rm A}$ is almost perfect, the frequencies show a shift of 25 μHz with respect to the values determined by Bouchy & Carrier (2002). On the other hand, sets of parameters with a better fit of the radii reduce significantly the shift of frequencies.

The small separation for the A component (Fig. 3) suggest that seismic observables would privilege younger models, whereas one of the two values of $\delta\nu_{\rm B}$ ($n = 23$) and the classical observables tend to a high value of the age. In fact, in our calibration (Ans, Bns) where only classical observable

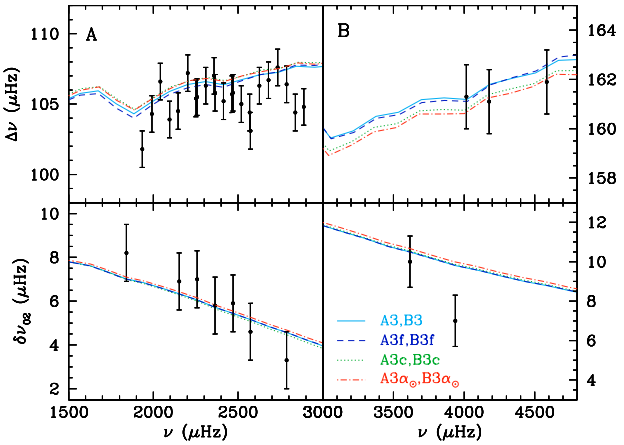

Fig. 4. As Fig. 3 but for models computed using different approach for convection: MLT with two mixing length parameters (solid line); FST (dashed lines); MLT with $\alpha_A = \alpha_B$ (dotted lines); and MLT with $\alpha_A = \alpha_B = \alpha_\odot$ (dash-dotted lines) Large and small separations are derived from stellar models, but the fitting is performed using the ratios r_{02} for component A and $\Delta\nu$ for component B.

have been taken into account for the fit, we obtain a very good agreement for masses, radii, luminosity and effective temperature (not taken as observable) for both components, and the age is $\tau = 8.9 \pm 1.8$ Gyr.

Although the small separation averaged value of component A is well reproduced by our models, the slope of $\delta\nu$ as a function of ν differs from the theoretical prediction. One could argue that this could be a consequence of taking as observable the average value of $\delta\nu$. Roxburgh & Vorontsov (2003, and references therein), show that the Tassoul asymptotic result gives a poor fit both to the small separations of stellar models and to the observed values for the Sun, and that a better fit is obtained by using the ratios of small and the large separations ($r_{02}(n)$). This ratio depends only on the inner phase shifts which are determined solely by the interior structure of the star and are uninfluenced by the unknown structure of the outer layers.

We have performed a similar fitting using six observational values of the ratio r_{02} as seismic constraints for the A component. Unfortunately, the p-modes identified for B component do not allow us to define any value of r_{02}; we decided, therefore, to take as the seismic constraint the average large separation. The first thing to be noticed, when comparing the new set of parameters (A3, B3) with the one based on average large and small separation for both components (A2, B2), is a difference in the resulting age of about 1 Gyr. We also see that by fitting r_{02}, we get a good fit of $\delta\nu_{02}$ for both stars (Fig. 4). The large separation is slightly higher than the observational one, as we obtained in (A2, B2) and (A1r, B1r).

In Fig. 6 we can see also the effect on the p-mode frequencies, the model (A3, B3) providing a better fit to the observational ones than the model (A2, B2).

Notice that the parameter set (A3, B3) was determined without taking into account the small separation for the B component. Theoretical $\langle\delta\nu\rangle$ is $\sim$10.15 μHz, that is close to the new observational value (10.1 μHz) by Kjeldsen & Bedding (2004). We wonder whether the high age obtained by taking $\langle\delta\nu_B\rangle$ as given by the average of two points (Carrier & Bourban 2003) is only a consequence of the low value imposed to $\langle\delta\nu_B\rangle$. In fact, a different calibration performed using the small and large separations as observables, but taking only $\delta\nu_B(n = 21)$ instead of the average of two available values, provides an age of 6.0 Gyr, in good agreement with r_{02} (A3, B3) fittings, and quite younger than (A2, B2) models.

Finally, we have also used r_{02} but without varying the masses. Again, the age is of the order of 6.0 Gyr, but now, the mixing-length parameters needed for both stars are quite different (by 17%).

The fits reported in Table 3 could indicate an inconsistency between the seismic and classical observables. Actually for component B the resulting radii are larger than the observed ones by more than $\sim 1\sigma$ or $\sim 2\sigma$ and the masses are smaller by more than $\sim 1\sigma$ or $\sim 2\sigma$ with respect to the values observationally derived. These results could be interpreted as a systematic error in the radii and/or in the mass determination. A calibration performed with a free M_B parameter/observable, leads to $M_B = 0.911\ M_\odot$ and $R_B = 0.863\ R_\odot$. The other parameters do not significantly change. This mass value would imply a systematic error of $\sim 4\sigma$ that, given the available high precision data, does not seem reliable. On the other hand, if R_B is left free, the fit of the other observables provides $R_B = 0.871\ R_\odot$ instead of 0.863 $R_\odot$, and a M_B value within 1 σ from the observed one. However, these fits have $\Delta\nu_B$ included in the χ^2 functional. To check if the large radius is only a consequence of $\Delta\nu_B$, we calibrate the system adopting as seismic constraints $r_{02}(n)$ for component A, and $\delta\nu(n = 21)$ for component B. In this case we are able to fit the radii and masses of both components within 1σ, but $\langle\Delta\nu_B\rangle$ is more than +3-σ away from the observational value, and the predicted frequencies are $\sim$40 μHz larger than observed ones. A priori, we cannot rule out a larger uncertainty in the observed radius. In the observational radius determination there is an implicit definition of stellar radius (that is not necessarily the same as the one used in stellar modelling) and an assumption about the limb darkening law and the atmosphere models. How much is the stellar radius affected by these assumptions? Kervella (2005, private communication) claims that these effects are much smaller than other errors intrinsic to the measurement method and already taken into account. So, more precise seismic data for αCenB are needed to understand this apparent inconsistency.

5.2. Effect of the treatment of convection

It is well known that one of the weak points of stellar evolution models is the treatment of convection. The "standard model" of convection adopted in stellar evolution is the mixing length theory (MLT) where turbulence is described by a relatively simple model that contains essentially one adjustable parameter: the mixing length $\Lambda = \alpha H_p$ (H_p being the local pressure scale height and α an unconstrained parameter). The value of this parameter determines the radius of the star and the behavior of the super-adiabatic region in the outer boundary of the stellar convective zone. The calibration of a stellar code using the solar

radius and solar luminosity provides the value of the mixing-length parameter ($\alpha_\odot$) which in turn is usually used to model other stars with the same physics. A question arises: can stars of different masses, initial chemical composition and evolutionary status be modeled with a unique α? If the answer is negative, how reliable is the shape of the isochrones determined with a unique α?

αCen offers a unique opportunity of testing our assumption about α and, therefore, our simplified way of overcoming the complex problem of convection in stars. The question of the universality of the mixing-length parameter has been approached many times in the past (Noels et al. 1991; Edmonds et al. 1992; Lydon et al. 1993; Neuforge 1993; Morel et al. 2000; Fernandes & Neuforge 1995; Guenther & Demarque 2000). Some attempts of calibrating αCen A and B in luminosity and radii using MLT theory suggest different values of α for each component and different from the $\alpha_\odot$, while others favor similar values for both components, or conclude that the uncertainties in masses and radii as well as the chemical composition should be reduced significantly before being able to draw firm a conclusion on whether the MLT parameter is unique or not (Lydon et al. 1993; Andersen 1991; Guenther & Demarque 2000). Nowadays, the high precision with which we know masses and radii for αCen A and B allows to analyze again this problem. The frequencies are very sensitive to R and therefore to α, and the difference between the observed frequencies ($\nu_{\rm obs}$) and the theoretical ones ($\nu_{\rm theo}$) is highly affected by how the super-adiabatic zone is described (see e.g. Schlattl et al. 1997).

In order to analyze these questions we have made several fits of the αCen observable quantities by using MLT with i) $\alpha_{\rm A} \neq \alpha_{\rm B}$ as free parameters; ii) $\alpha_{\rm A} = \alpha_{\rm B}$ free parameter; and iii) $\alpha_{\rm A} = \alpha_{\rm B} = \alpha_\odot$ fixed; and iv) since Morel et al. (2000) presented also controversial results when comparing calibrations for αCen using MLT or FST, we shall analyze as well the effect of using the FST treatment of convection.

5.2.1. MLT versus FST

Mimicking the spectral distribution of eddies by one "average" eddy, such as MLT theory does, has critical consequences on the computation of MLT fluxes. Canuto (1996) shows that in the limit of highly efficient convection MLT underestimates the convective flux, and on the contrary, in the low efficiency limit, MLT overestimates the convective flux. FST models attempt to overcome the one-eddy approximation by using a turbulence model to compute the full spectrum of a turbulent convective flow. As consequence, the convective flux is ~10 times larger than the MLT one in the limit of high efficiency, and ~0.3 in the limit of low efficiency. This behavior yields, in the super-adiabatic region at the top of a convective zone, steeper temperature gradients for FST than for solar-tuned MLT. The mixing length used in FST treatment is in general defined as the distance from a given point to the boundary of the convective zone. However, the FST fluxes have also been used combined with other definitions of mixing length. For instance, Bernkopf (1998), use the FST fluxes with a mixing length $\Lambda = \alpha^* H_{\rm p}$ with $\alpha^* < 1$. Morel et al. (2000) use also this kind of description of FST convection with CM91 for the fluxes. Here we will use this prescription of FST treatment of convection, with the fluxes by Canuto et al. (1996) instead of CM(91, 92). The main difference is in the temperature gradient, steeper in CM than in CGM96, but both, in any case, much steeper than the MLT one. Morel et al. (2000) found significant differences in the fitted parameters (in particular a 1.5 Gyr difference in the age) when investigating the effect of using a different theory of convection in the modelling of α Centauri. This is rather surprising since the treatment of convection affects only the very external layers of the star, and such an important effect on the age of the star is not expected.

The convection parameters that result from our fits are, as in the case of the calibration with MLT, close to the parameter needed to calibrate the Sun (0.753). Furthermore, in comparing the models (A3, B3) with (A3f, B3f) ones, we do not observe any difference in the parameters of the models fitting the system αCen using MLT or FST. In principle this is a logical behavior since we considered as the seismological observable the $r_{02}(n)$ (Roxburgh & Vorontsov 2003) ratio, and this quantity is independent of surface properties of the model. However, also the sets of parameters (A2, B2) and (A2f, B2f) determined by using large and small frequency separations as constraints are in fact the same, independent of the convection description used.

We would expect, as in the Sun, a decrease of the difference between theoretical and observational frequencies in the high frequency domain when FST is used. However, for our binary system, the improvement provided by FST treatment with respect to MLT is quite small.

For αCen A the improvement is of the order of 4 μHz at 3000 μHz, while for the B component, this effect does not appear clearly (Fig. 6). In fact, the difference between MLT and FST frequencies is due to a different radius and mass. If we adopt for $M_{\rm B}$ and $R_{\rm B}$ the values determined in the calibration B3 as the real ones, and compute a new FST calibration, we find that the difference between the MLT and FST frequencies in the observational domain (3000–4600 μHz) goes from 0 to 3 μHz, while the difference in frequencies between B3 and B3f introduced by the different mass and radius is of the order of 8 μHz.

5.2.2. One or two different values for the mixing length parameter?

Several times in the literature the question has been addressed of whether convection in the two components of α Centauri should be described with distinct mixing-length parameters and, if, given the observational uncertainties, the inferred difference between mixing length parameters is significant (see e.g. Eggenberger et al. (2004), where an exhaustive review of previous calibrations is also presented). It was, in fact, already suggested in Guenther & Demarque (2000) that a reduction in the observational uncertainties and the inclusion of seismic constraints in the modelling would allow a more robust inference on the mixing-length parameters of αCen A and B. This is now the case, thanks to the detection of solar-like oscillations

and to the precise determination of radii. These are compatible with effective temperatures spectroscopically determined and significantly reduce the error box in the HR diagram. As a general result of the calibrations presented in the previous sections we find that the mixing-length parameter of the calibrated model A ($\alpha_{\rm A}$) is approximately 5–10% smaller than $\alpha_{\rm B}$.

Numerical simulations of convection have permitted us to carry out a calibration of the mixing-length parameter through the HR diagram. A function $\alpha(T_{\rm eff}, \log g)$ is determined to reproduce the step of the specific entropy provided by the atmosphere hydrodynamic models. Both calibrations, the one by Ludwig et al. (1999) (based on 2-D simulations) and the one by Trampedach (2004) (based on 3-D simulations) show slight variations of α with the position in the HR diagram, and suggest that the mixing parameter should be represented as a function of $\log T_{\rm eff}$, $\log g$ and chemical composition.

Actually, comparing our results with these theoretical predictions, we see that the difference between the value determined for $\alpha_{\rm B}$ and $\alpha_{\rm A}$ is in good agreement with the predictions by numerical simulations of convection. Moreover, our α values for the two components bracket that obtained by calibrating the Sun ($\alpha_\odot = 1.91$) with the same physics (see for instance the model A3, B3). This is what one expects from their HR location and from the calibrations by Ludwig et al. (1999) and Trampedach (2004). We note, however, that in the fits obtained by using $\langle\Delta\nu\rangle$ and $\langle\delta\nu\rangle$ we find $\alpha_{\rm B} > \alpha_{\rm A}$, but also $\alpha_{\rm A}$ larger than the solar one. The difference with respect to the solar value is even larger when the masses of the components are assumed to be fixed. The same effect is present in Eggenberger et al. (2004): they find $\alpha_{\rm B} > \alpha_{\rm A}$, but their values are far from their solar one.

In order to determine whether the addition of an extra free parameter leads to a significant improvement of the fit, we performed a calibration assuming a single mixing-length parameter for both components, and including the $r_{02}(n)$ ratios in the quality function (A3c, B3c). The value of α for this calibration is $\alpha = 1.95$ (quite close to the solar one), but the masses now are slightly larger for the component A, and slightly smaller for the component B. The same happens if we decide to fix $\alpha_{\rm A} = \alpha_{\rm B} = \alpha_\odot$. The masses are within 2σ of the observed value, and the age is the same, $\tau = 5.7 - 5.8$ Gyr.

A different result is obtained if the small and large differences are considered in the quality function (A2c, B2c), and the mixing-length parameter is assumed to be the same for both stars. In this case, the value reached ($\alpha = 1.78$) is not so close to the solar one, $M_{\rm B}$ must decrease to 0.919 $M_\odot$, and the age of the system decreases with respect to the value obtained allowing two different mixing-length parameters. This result recalls that obtained by Thévenin et al. (2002), who using a unique α had to decrease the $M_{\rm B}$ to 0.907 $M_\odot$.

Since adding a free parameter would naturally lead to a better fit (a lower χ^2 as defined in Eq.(1)), for a quantitative comparison between the quality of the fit obtained with a different number of model parameters, it is more meaningful to compare the so-called "reduced" $\chi^2_{\rm R}$ (Eq. (4)). As can be seen in Table 3 the value of χ^2_R is lower if two distinct mixing length parameters are used in the modelling (both comparing A3, B3 with A3c, B3c and A2, B2 with A2c, B2c): this suggests that, with the adopted observational constraints, the addition of another free mixing-length parameter is justified. In fact, comparing the fits obtained with one or two mixing-length parameters, the F-test gives a confidence of 85–90% that the inclusion of two different parameters for convection is significant. We should however recall that such a statistical test, and generally the χ^2 statistics, assumes that the observational errors are distributed about the mean following a Gaussian distribution. This is not necessarily true as systematic shifts in the observed quantities and inaccuracies in the models cannot be excluded. As could also be expected, the uncertainties adopted with the observational constraints are crucial. For instance, we find that if the observational error in the mass of the component B is doubled, the addition of a second free parameter for convection is no longer justified.

5.3. Disentangling the physics

One of the principal motivations for pursuing the study of pulsations in other stars is to test the assumptions concerning the physics underlying the stellar structure theory. To practically investigate this idea, we compute four models of αCen that use the same observational constraints and model parameters as the reference calibrations (A3, B3) and (A1r, B1r), but incorporate changes in the physical assumptions. These are: CEFF EoS (A1e, B1e; A3e, B3e), Asplund et al. (2004) chemical composition (A5, B5). To test the effects of gravitational settling we have calibrated the models (A1nd, B1nd) and (A3nd, B3nd) without microscopic diffusion.

The central question is whether the residual errors are observationally significant. If the residuals are all small compared to the observational errors, it is not possible to distinguish parameter changes from changes in physical assumptions. In general, we find that stars obeying different physics succeed remarkably well in masquerading as stars that merely have different parameters (Brown et al. 1994).

5.3.1. Equation of state

Concerning the equation of state, the calibration assuming CEFF (A3e, B3e) leads to a result in agreement with the fit (A3, B3) computed adopting OPAL01, both in terms of $\chi^2_{\rm R}$ (either the total one or that corresponding at each observable quantity), and of the fitted parameters. This is expected for stars with an internal structure similar to the sun: as shown by Miglio (2004) the differences between the sound speed and the first adiabatic exponent (Γ_1), due solely to the use of a different EOS (CEFF and OPAL01), are smaller than 1% except in outer regions with radii larger than 0.95 R_*, that is of the same order of those predicted in solar models (see e.g. Basu & Christensen-Dalsgaard 1997). The differences appear to be larger in the lower-mass model B than in model A, and are mainly located in the hydrogen and helium ionization regions. In that study, the differences in Γ_1 came from the application of CEFF or OPAL01 to a given stellar structure ($\log\rho$ vs. $\log T$) and chemical composition. In the calibration procedure, such small differences in the internal structure of a model propagate in a variation of the

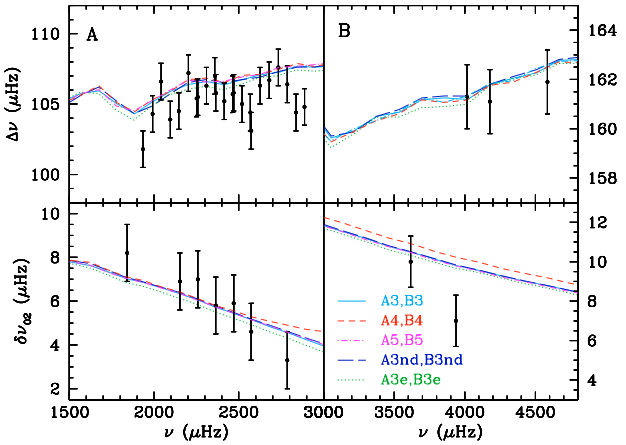

Fig. 5. As Fig. 4 but with different curves corresponding to different physics included in the stellar computation: convective overshooting (dashed lines); solar mixture from Asplund et al. (2004) instead of Grevesse & Noels (1993)(dash-dotted lines); no gravitational settling (solid lines); CEFF equation of state instead of OPAL01 (dotted lines).

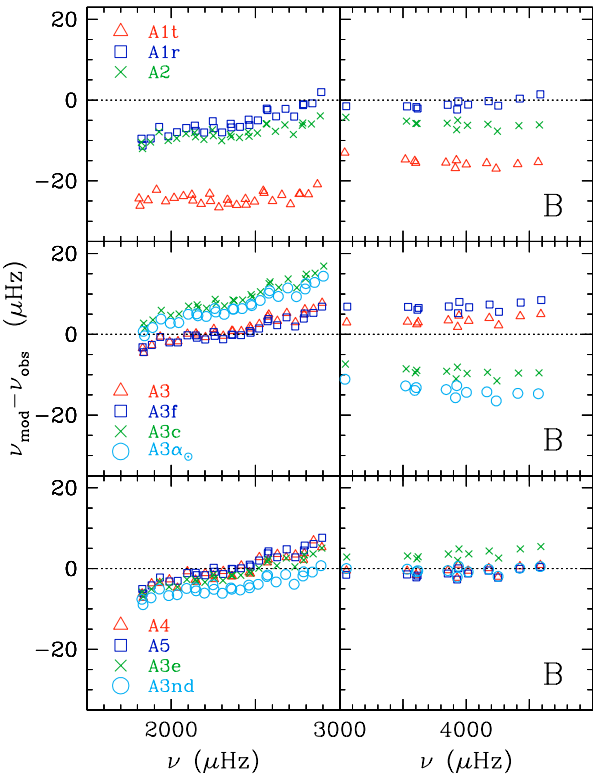

Fig. 6. Difference between theoretical and observed frequencies for the sets of parameters whose separations have been plotted in Fig. 3 (*upper panel*); in Fig. 4 (*middle panel*); and Fig 5 (*lower panel*). Left side corresponding to αCen A, and right side to αCen B. The labels correspond to the identification of the model used in Table 2.

observables of each model that could be easily compensated by a re-adjustment of the free parameters.

The models calibrated by using different equations of state are very similar. There is, nevertheless, a difference in the frequencies. In Fig. 7 (solid lines) we plot the difference between (A3, B3) and (A3e, B3e) frequencies. The upper panel corresponds to the A component, and the lower panel to the

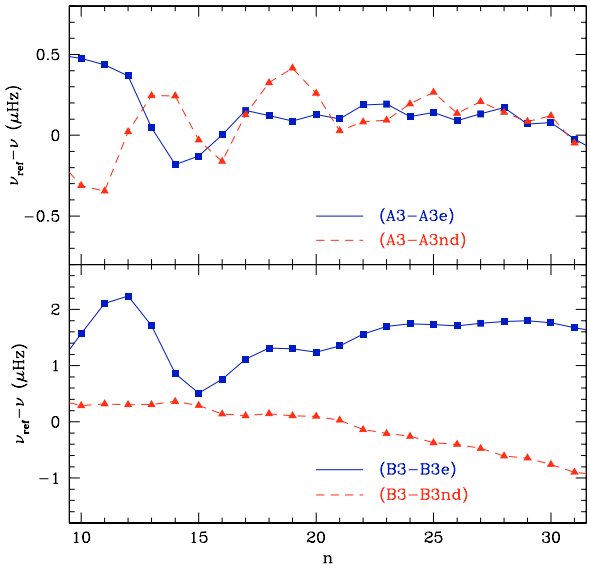

Fig. 7. Difference of frequencies between a reference calibration (A3, B3), and both, that with a different EoS (A3e, B3e) (solid lines), and without microscopic diffusion (A3nd, B3nd) (dahsed lines). Upper panel corresponds to component A, and lower panel to component B.

B one. This difference in frequencies shows a behavior depending on ν with an oscillatory signature. This is expected for instance, when the models have either different locations of the convective region boundaries, or a different behaviour of Γ_1. The bottom of the convective zone in αCen A is located at $x_{\rm zc} = R_{\rm cz}/R_* = 0.707$ for A3 calibration, and $x_{\rm zc} = 0.711$ for A3e model. Therefore, the oscillatory signature is probably related to the changes in the second helium ionization zone. The amplitude of this oscillation is linked to the difference in depth of the Γ_1 bump, and the period contains information about the location of the difference in stellar structure. For star A, the amplitude of the oscillation between the order $n = 10$ and 15 is around 0.7 μHz, while for the B component that is almost 2 μHz.

5.3.2. Microscopic diffusion

The calibrations without diffusion (A1nd, B1nd) and (A3nd, B3nd) provide fits of similar quality with respect to the corresponding calibrations including gravitational settling, respectively (A1r, B1r) and (A3, B3). As reported in Table 2 the parameters resulting from the calibrations differ, as expected, in the initial chemical composition. The smaller mass fraction of He required in these calibrations implies also a slight increase in the age of the system: 6.3 ± 0.4 Gyr for (A3nd, B3nd) versus 5.8 ± 0.2 Gyr for (A3, B3) (and 7.1 ± 0.6 Gyr for (A1nd, B1nd) versus 6.8 ± 0.5 Gyr for (A1r, B1r)). The (A3nd, B3nd) calibration is consistent with the one obtained by Thoul et al. (2003). Since they use only αCen A frequencies, their age estimation is not affected by the low $\delta\nu$(B) value.

The mixing-length parameters are also re-adjusted to fit the stellar radius, and also in this case $\alpha_{\rm B}$ is almost 8% larger than $\alpha_{\rm A}$, and both bracket the mixing length parameter obtained for a Sun calibrated without microscopic diffusion ($\alpha_\odot = 1.84$).

In Fig. 7 (dashed-line) we show how diffusion affects the frequencies. We plot the residuals defined as ν_{n0}(A3) − ν_{n0}(A3nd) (upper panel) and ν_{n0}(B3)−ν_{n0}(B3nd) (lower panel). For component A the residuals as function of the order n show an oscillatory behavior, reflecting the changes in envelope He abundance (Y_s). Actually the calibrated model including diffusion has a superficial He abundance Y_s(A3) = 0.245, while model A3nd, without gravitational settling has Y_s = 0.270.This difference implies as well a different opacity and, therefore, a different location of the boundary of the convective zone (X_{cz}(A3nd) = 0.725). To avoid changing the figure scale, the curve of residuals in the upper panel has been shifted down by 2.5 μHz; we see that the amplitude of the oscillatory signal is around 0.5 μHz between n = 10 and n = 20.

For component B the curve of residuals shows a completely different behavior. Since αCen B is less massive than its companion, the mass contained in its convective zone is much larger and, therefore, the effect of microscopic diffusion is much smaller. The value of Y_s for B3 is less than 4% smaller than that for B3nd, while for the component A, the difference in Y_s between both calibrations (A3 and A3nd) is around 10%.

5.3.3. Solar mixture

Asplund et al. (2004) have recently proposed a substantial revision of the abundance of C N and O in the solar photosphere. Since the value of the surface metallicity of αCen is observationally determined relative to the solar heavy element abundance, the solar $(Z/X)_s$ = 0.0177 resulting from the new solar calibration would lower $(Z/X)_s$ in αCen by ∼30%. We thus calibrate our models assuming as observational constraint $(Z/X)_s$ = 0.029 (instead of 0.039) and using in the computations OPAL opacity tables calculated with the solar mixture proposed by Asplund et al. (2004). The results of this calibrations, models (A5, B5), present a different initial chemical composition, but no other significant deviation from the global parameters of models (A3, B3) is noticed. As it happens for the Sun, the αCenA model calibrated with Grevesse & Noels (1993) has a deeper convective region compared with the model A5, but the uncertainty in the observational data is larger than in the Sun, and this difference can be masked by other choices of parameters.

5.3.4. Overshooting

An additional consequence of our simple way of describing convection in stellar models is the need to parameterize convective overshooting. In general (see e.g. Schaller et al. 1992) convective core overshooting is necessary to fit isochrones of open clusters for masses larger than a given critical mass. The problem is to determine this critical mass and to describe the transition between no-overshooting mass domain and overshooting mass domain. On the one hand, the mass and effective temperature of αCen A are quite close to solar values, and one could think that no overshooting should be introduced. Nevertheless the chemical composition of αCen A is different from the solar one and the evolution of a convective core does not necessarily show the same behaviour. The mass of αCen places it in the boundary region between models with and without a convective core. We have made several calibrations varying the thickness of the overshooting layer $ov = \beta * (\min(r_{cv}, H_p(r_{cv})))$ (where r_{cv} is the radius of the convective core) with β from 0.0, 0.1, 0.15 and 0.2. In fact, for values of $\beta \leq 0.15$ no convective core remains after the PMS, therefore the parameters resulting from the fitting are not changed.

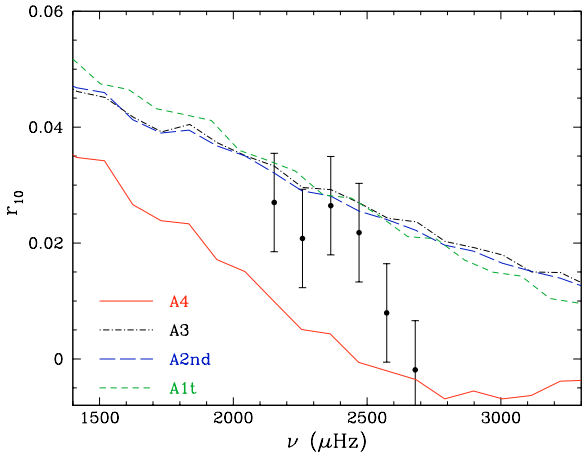

Fig. 8. $r_{10}(n)$ ratios for A component. Points represent the observational values with their error bars assuming an error in frequencies equal to 2σ. Short-dashed line corresponds to the model calibrated using large and small separation in the χ^2 functional, as well as the effective temperatures instead of the radii. The other three curves correspond to modes calibrated using $r_{02}(n)$ in χ^2: model including overshooting (solid line) and presenting a convective core; the same calibration without overshooting (dot-dashed line), and calibration without overshooting and without microscopic diffusion (long-dashed line).

In Tables 2 and 3 we report the set of parameters and observables corresponding to models (A4, B4) calibrated with β = 0.2. As should be expected, including overshooting reduces the age of the system. Figure 5 shows the large and small separations. We find a possible direct indicator of a convective core in the behavior of the small separation of component A at high frequencies (ν > 2500 μHz). That is even more evident in the signature left in r_{02}. However, given the uncertainty (1.3 μHz) affecting the p-modes involved in the highest frequency $r_{02}(n)$ (or $\delta\nu(n)$), it is not possible, based only on $r_{02}(n)$ or $\delta\nu_{02}$, to rule out a convective core in αCen A. The ratio $r_{10}(n) = (\nu_{n0} - 2\nu_{n1} + \nu_{n+1,0})/(2\Delta\nu_0(n+1))$, however, is much more eloquent, as shown in Fig. 8, and *allows us to reject model A4: current observational constraints seem not to be in favour of a convective core in αCen A*.

6. Summary and conclusions

We propose a calibration of the binary system αCen by means of the Levenberg-Marquardt minimization algorithm applying it simultaneously to classical (photometric, spectroscopic and astrometric) and seismic observables. The main features of this sort of algorithm make it an ideal tool for the aim of this work: to practically analyze the effectiveness of oscillation frequencies in constraining stellar model parameters and

stellar evolution physics, by using the p-modes identified by Bouchy & Carrier (2002) (αCen A) and by Carrier & Bourban (2003)(αCen B). Actually thanks to its low computational cost, this algorithm allows one to search for the best model in the full 7-dimensional parameter space describing the binary system, varying both the set of stellar observables and the physics included in stellar modelling.

As a starting point we assumed the same observables as Eggenberger et al. (2004). In spite of the different EoS (MHD), diffusion treatment (Richard et al. 1996, for five elements separately), cross section of nuclear reactions (NACRE) and atmospheric boundary conditions, we derive a set of stellar parameters (A1r, B1r) in complete agreement with theirs.

By comparison between calibrations with different observables we make clear that care has to be taken when using $\Delta\nu_0$ to constrain fundamental stellar parameters. Given the strong dependence of $\Delta\nu_0$ on surface layers, and our poor understanding of the physics describing outer stellar regions, seeking a perfect agreement between observed and predicted $\Delta\nu_0$, may bias our results toward, for instance, inaccurate radii. This is clear when comparing the models A1t and A1r; in the former a perfect agreement with the observed $\Delta\nu$ is reached but the radii (and the frequencies, see Fig. 6) deviate significantly from their observational values.

An additional source of systematic error in the calibrations concerns the value of the small frequency separation of component B. Since the observational data are still rather poor one of the two measured values, $\delta\nu_{\rm B}(n = 23)$ leads to a higher age than suggested by $\delta\nu_{\rm A}$.

The value of $\delta\nu_{\rm B}$ predicted in our calibration (A3, B3) (where $\delta\nu_{\rm B}$ is not included in the χ^2) is in agreement with $\delta\nu_{\rm B}(n = 21)$ and with the very recent value published by Kjeldsen & Bedding (2004). This also suggests that sufficiently precise seismic data of one star are sufficient to determine fundamental parameters of the system. In fact additional calibrations, not shown in Table 2, where no seismic constraints of component B are included, lead to fitted parameters compatible with e.g. (A3, B3) even though a large discrepancy between predicted and observed frequencies of αCen B is observed.

We therefore propose to use r_{02} as a reliable seismic constraint to determine fundamental parameters of a star. The large frequency separation could, nonetheless, provide a first estimate of the mean density and, as shown e.g. in Gough (1990), an useful information on localized features in stellar interior once more accurate determinations of solar-like oscillations will be available.

Section 5.2 was devoted to the study of the effects on the calibration of our uncertainties concerning stellar convection. If the calibrations, e.g. (A3, B3), are performed considering a free parameter describing convection in each component ($\alpha_{\rm A}$, $\alpha_{\rm B}$) we find, as Eggenberger et al. (2004), $\alpha_{\rm B}$ 5–11% higher than $\alpha_{\rm A}$. Differently from Eggenberger et al. (2004) we find that $\alpha_{\rm A} < \alpha_\odot < \alpha_{\rm B}$: this is of primary relevance when making statements concerning the difference between $\alpha_{\rm A}$ and $\alpha_{\rm B}$, otherwise we would also have to justify an even bigger (not expected) difference between $\alpha_{\rm A}$ and $\alpha_\odot$. We notice also that our inferred values of α follow the same trend predicted by MLT parameter calibration based on 2D (Ludwig et al. 1999) and 3D (Trampedach 2004) hydrodynamic atmosphere models.

In order to draw more firm conclusions on the significance of considering $\alpha_{\rm A}$ and $\alpha_{\rm B}$ as free parameters we repeated our calibrations (A3, B3) and (A2, B2) assuming a single parameter for both components ((A3c, B3c) and (A2c, B2c)). The fit necessarily improves when an additional free parameter is introduced in the calibration, nevertheless we find, with the observational constraints we adopted, the difference between $\alpha_{\rm A}$ and $\alpha_{\rm B}$ significant. We note also that the value of α obtained in (A3c, B3c) and (A2c, B2c) calibrations is quite close to the corresponding $\alpha_\odot$.

We also find that, contrary to what was obtained by Morel et al. (2000), the use of a different theory of convection (MLT or FST) in our models does not change the set of parameters derived from the fitting. The only effect of convection model is a slight improvement in the fit of high frequencies when using FST (in particular for A component).

The available seismic data are not in favour of a convective core in α Cen A, moreover, the overshooting parameter needed for a convective core to persist after the PMS ($\beta = 0.2$) appears to be too large for a model of the mass and chemical composition of α Cen A (see e.g. Demarque et al. 2004).

Finally, we find that stars obeying different physics provide similar fits to those obtained with stars that merely have different parameters. As a consequence, we are not able from present data to discriminate either between different EoS, or between diffusion or diffusion-free models. Figure 7 shows, however, that expected precision from space missions would allow us to apply inversion techniques to frequency data. Adding seismic observables has significantly improved the determination of the system fundamental parameters, but more precise observations are needed to be able to extract information about the internal structure of the stars.

Acknowledgements. A.M. and J.M. acknowledge financial support from the Prodex-ESA Contract 15448/01/NL/Sfe(IC). A.M. is also thankful to Teresa Teixeira for her useful suggestions.

References

Alexander, D. R., & Ferguson, J. W. 1994, ApJ, 437, 879
Andersen, J. 1991, A&ARv, 3, 91
Asplund, M., Grevesse, N., Sauval, A. J., Allende Prieto, C., & Kiselman, D. 2004, A&A, 417, 751
Asplund, M., Grevesse, N., Sauval, A. J., Allende Prieto, C., & Blomme, R. 2005, A&A, 431, 693
Böhm-Vitense, E. 1958, Zeitschrift Astrophys., 46, 108
Baglin, A., & The COROT Team. 1998, in New Eyes to See Inside the Sun and Stars, IAU Symp., 185, 301
Basu, S., & Christensen-Dalsgaard, J. 1997, A&A, 322, L5
Basu, S., Christensen-Dalsgaard, J., Chaplin, W. J., et al. 1997, MNRAS, 292, 243
Bernkopf, J. 1998, A&A, 332, 127
Bevington, P. R., & Robinson, D. K. 2003, Data Reduction and Error Analysis for the Physical Sciences (McGraw-Hill)
Bouchy, F. 2002, in ASP Conf. Ser., 474
Bouchy, F., & Carrier, F. 2002, A&A, 390, 205
Brown, T. M., Christensen-Dalsgaard, J., Weibel-Mihalas, B., & Gilliland, R. L. 1994, ApJ, 427, 1013

Burgers, J. M. 1969, Flow Equations for Composite Gases, Flow Equations for Composite Gases (New York: Academic Press)
Canuto, V. M. 1996, ApJ, 467, 385
Canuto, V. M., Goldman, I., & Mazzitelli, I. 1996, ApJ, 473, 550
Canuto, V. M., & Mazzitelli, I. 1991, ApJ, 370, 295
Canuto, V. M., & Mazzitelli, I. 1992, ApJ, 389, 724
Carrier, F., & Bourban, G. 2003, A&A, 406, L23
Caughlan, G. R., & Fowler, W. A. 1988, Atomic Data and Nuclear Data Tables, 40, 283
Chmielewski, Y., Friel, E., Cayrel de Strobel, G., & Bentolila, C. 1992, A&A, 263, 219
Christensen-Dalsgaard, J., & Däppen, W. 1992, A&ARv, 4, 267
Christensen-Dalsgaard, J., Bedding, T. R., Houdek, G., et al. 1995, in ASP Conf. Ser., 447
Christensen-Dalsgaard, J., Dappen, W., Ajukov, S. V., et al. 1996, Science, 272, 1286
Cox, J. P., & Giuli, R. T. 1968, Principles of Stellar Structure (Gordon and Breach)
Demarque, P., Woo, J., Kim, Y., & Yi, S. K. 2004, ApJS, 155, 667
Di Mauro, M. P., Christensen-Dalsgaard, J., Kjeldsen, H., Bedding, T. R., & Paternò, L. 2003, A&A, 404, 341
Edmonds, P., Cram, L., Demarque, P., Guenther, D. B., & Pinsonneault, M. H. 1992, ApJ, 394, 313
Eggenberger, P., Charbonnel, C., Talon, S., et al. 2004, A&A, 417, 235
Fernandes, J., & Neuforge, C. 1995, A&A, 295, 678
Flannery, B. P., & Ayres, T. R. 1978, ApJ, 221, 175
Gough, D. O. 1990, Lecture Notes in Physics (Berlin: Springer Verlag), 367, 283
Grevesse, N., & Noels, A. 1993, in La formation des éléments chimiques, AVCP, ed. R. D. Hauck B., Paltani S.
Guenther, D. B., & Brown, K. I. T. 2004, ApJ, 600, 419
Guenther, D. B., & Demarque, P. 2000, ApJ, 531, 503
Iglesias, C. A., & Rogers, F. J. 1996, ApJ, 464, 943
Kervella, P., Thévenin, F., Ségransan, D., et al. 2003, A&A, 404, 1087
Kjeldsen, H., & Bedding, T. R. 1995, A&A, 293, 87
Kjeldsen, H., & Bedding, T. R. 2004, in ESA SP-559: SOHO 14 Helio- and Asteroseismology: Towards a Golden Future, 101
Kurucz, R. L. 1998, http://kurucz.harvard.edu/grids.html
Ludwig, H., Freytag, B., & Steffen, M. 1999, A&A, 346, 111
Lydon, T. J., Fox, P. A., & Sofia, S. 1993, ApJ, 413, 390
Matthews, J. M. 1998, in Structure and Dynamics of the Interior of the Sun and Sun-like Stars SOHO 6/GONG 98 Workshop Abstract, June 1-4, 1998, Boston, Massachusetts, 395
Metcalfe, T. S. 2005, e-prints [ArXiv:astro-ph/0501421]
Miglio, A. 2004, in Equation-of-State and Phase-Transition in Models of Ordinary Astrophysical Matter, AIP Conf. Proc., 731, 187
Morel, P., Provost, J., Lebreton, Y., Thévenin, F., & Berthomieu, G. 2000, A&A, 363, 675
Neuforge, C. 1993, A&A, 268, 650
Neuforge-Verheecke, C., & Magain, P. 1997, A&A, 328, 261
Noels, A., Grevesse, N., Magain, P., et al. 1991, A&A, 247, 91
Pijpers, F. P. 2003, A&A, 400, 241
Pourbaix, D., Nidever, D., McCarthy, C., et al. 2002, A&A, 386, 280
Richard, O., Vauclair, S., Charbonnel, C., & Dziembowski, W. A. 1996, A&A, 312, 1000
Rogers, F. J., & Nayfonov, A. 2002, ApJ, 576, 1064
Roxburgh, I. W., & Vorontsov, S. V. 2003, A&A, 411, 215
Söderhjelm, S. 1999, A&A, 341, 121
Salpeter, E. E. 1954, Aust. J. Phys., 7, 373
Schaller, G., Schaerer, D., Meynet, G., & Maeder, A. 1992, A&AS, 96, 269
Schlattl, H., Weiss, A., & Ludwig, H.-G. 1997, A&A, 322, 646
Tassoul, M. 1980, ApJS, 43, 469
Thévenin, F., Provost, J., Morel, P., et al. 2002, A&A, 392, L9
Thoul, A., Scuflaire, R., Noels, A., et al. 2003, A&A, 402, 293
Thoul, A. A., Bahcall, J. N., & Loeb, A. 1994, ApJ, 421, 828
Trampedach, R. 2004, Ph.D. Thesis
Turcotte, S., Richer, J., Michaud, G., Iglesias, C. A., & Rogers, F. J. 1998, ApJ, 504, 539